

Co-extruded mechanically tunable multilayer elastomer laser

Guilin Mao,¹ James Andrews,^{1,*} Michael Crescimanno,¹ Kenneth D. Singer,^{2,3} Eric Baer,³ Anne Hiltner,³ Hyunmin Song,³ Bijayandra Shakya¹

¹Department of Physics and Astronomy, Youngstown State University, Youngstown, Ohio 44555 USA

²Department of Physics, Case Western Reserve University, Cleveland, Ohio 44106 USA

³Department of Macromolecular Science, Case Western Reserve University, Cleveland, Ohio 44106 USA

*jandrews@ysu.edu

Abstract: We have fabricated and studied mechanically tunable elastomer dye lasers constructed in large area sheets by a single-step layer-multiplying co-extrusion process. The laser films consist of a central dye-doped (Rhodamine-6G) elastomer layer between two 128-layer distributed Bragg reflector (DBR) films comprised of alternating elastomer layers with different refractive indices. The central gain layer is formed by folding the coextruded DBR film to enclose a dye-doped skin layer. By mechanically stretching the elastomer laser film from 0% to 19%, a tunable miniature laser source was obtained with ~50 nm continuous tunability from red to green. Optically pumped by a frequency-doubled Nd:YAG laser, the elastomer laser showed a lasing threshold of 0.9 mJ/cm² at 600 nm.

©2011 Optical Society of America

OCIS codes: (140.3600) Tunable lasers; (160.5470) polymer; (140.2050) Dye lasers.

References and links

1. I. P. Ilchishin, "Generation of a tunable radiation by impurity cholesteric liquid-crystals," *JETP Lett.* **32**, 24–27 (1980).
2. F. Simoni, G. Cipparrone, and R. Bartolino, "Effect of tuning of a dye-laser induced by a liquid-crystal device," *Mol. Cryst. Liq. Cryst. (Phila. Pa.)* **1**, 3–4 (1985).
3. F. Simoni, G. Cipparrone, and R. Bartolino, "Tuning of a dye-laser by a liquid-crystal," *Mol. Cryst. Liq. Cryst. (Phila. Pa.)* **139**(1), 161–169 (1986).
4. H. Finkelmann, S. T. Kim, A. Munoz, P. Palffy-Muhoray, and B. Taheri, "Tunable Mirrorless Lasing in Cholesteric Liquid Crystalline Elastomers," *Adv. Mater. (Deerfield Beach Fla.)* **13**(14), 1069–1072 (2001).
5. J. Schmidtke, S. Kniesel, and H. Finkelmann, "Probing the photonic properties of a cholesteric elastomer under biaxial stress," *Macromolecules* **38**(4), 1357–1363 (2005).
6. A. Chanishvili, G. Chilaya, G. Petriashvili, R. Barberi, R. Bartolino, G. Cipparrone, A. Mazzulla, R. Gimenez, L. Oriol, and M. Pinol, "Widely tunable ultraviolet-visible liquid crystal laser," *Appl. Phys. Lett.* **86**(5), 051107 (2005).
7. G. Strangi, V. Barna, R. Caputo, A. De Luca, C. Versace, N. Scaramuzza, C. Umeton, R. Bartolino, and G. N. Price, "Color-tunable organic microcavity laser array using distributed feedback," *Phys. Rev. Lett.* **94**(6), 063903 (2005).
8. A. D. Ford, S. M. Morris, and H. J. Coles, "Photonics and lasing in liquid crystals," *Mater. Today* **9**(7-8), 36–42 (2006).
9. Z. Li, Z. Zhang, A. Scherer, and D. Psaltis, "Mechanically tunable optofluidic distributed feedback dye laser," *Opt. Express* **14**(22), 10494–10499 (2006).
10. L. M. Blinov, G. Cipparrone, V. V. Lazarev, P. Pagliusi, and T. Rugiero, "Liquid crystal as laser medium with tunable gain spectra," *Opt. Express* **16**(9), 6625–6630 (2008).
11. P. V. Shibaev, P. Rivera, D. Teter, S. Marsico, M. Sanzari, V. Ramakrishnan, and E. Hanelt, "Color changing and lasing stretchable cholesteric films," *Opt. Express* **16**(5), 2965–2970 (2008).
12. G. Petriashvili, M. A. Matranga, M. P. De Santo, G. Chilaya, and R. Barberi, "Wide band gap materials as a new tuning strategy for dye doped cholesteric liquid crystals laser," *Opt. Express* **17**(6), 4553–4558 (2009).
13. C. R. Lee, S. H. Lin, H. C. Yeh, and T. D. Ji, "Band-tunable color cone lasing emission based on dye-doped cholesteric liquid crystals with various pitches and a pitch gradient," *Opt. Express* **17**(25), 22616–22623 (2009).
14. F. Serra, M. A. Matranga, Y. Ji, and E. M. Terentjev, "Single-mode laser tuning from cholesteric elastomers using a "notch" band-gap configuration," *Opt. Express* **18**(2), 575–581 (2010).
15. W. Song and D. Psaltis, "Pneumatically tunable optofluidic dye laser," *Appl. Phys. Lett.* **96**(8), 081101 (2010).
16. M. R. Weinberger, G. Langer, A. Pogantsch, A. Haase, E. Zojer, and W. Kern, "Continuously color-tunable rubber laser," *Adv. Mater. (Deerfield Beach Fla.)* **16**(2), 130–133 (2004).

17. T. Kavc, G. Langer, W. Kern, G. Kranzelbinder, E. Toussaere, G. A. Turnbull, I. D. W. Samuel, K. F. Iskra, T. Neger, and A. Pogantsch, "Index and relief gratings in polymer films for organic distributed feedback lasers," *Chem. Mater.* **14**(10), 4178–4185 (2002).
18. G. Kranzelbinder, E. Toussaere, J. Zyss, T. Kavc, G. Langer, and W. Kern, "Organic surface emitting laser based on a deep-ultraviolet photopolymer containing thiocyanate groups," *Appl. Phys. Lett.* **82**(14), 2203–2205 (2003).
19. H. Song, K. Singer, J. Lott, Y. Wu, J. Zhou, J. Andrews, E. Baer, A. Hiltner, and C. Weder, "Continuously melt processing of all-polymer distributed feedback lasers," *J. Mater. Chem.* **19**(40), 7520–7524 (2009).
20. K. D. Singer, T. Kazmierczak, J. Lott, H. Song, Y. Wu, J. Andrews, E. Baer, A. Hiltner, and C. Weder, "Melt-processed all-polymer distributed Bragg reflector laser," *Opt. Express* **16**(14), 10358–10363 (2008).
21. T. Kazmierczak, H. Song, A. Hiltner, and E. Baer, "Polymeric one-dimensional photonic crystals by continuous coextrusion," *Macromol. Rapid Commun.* **28**(23), 2210–2216 (2007).
22. Y. Wu, K. D. Singer, R. G. Petschek, H. Song, E. Baer, and A. Hiltner, "Mode delocalization in 1D photonic crystal lasers," *Opt. Express* **17**(20), 18038–18043 (2009).
23. H. P. Wang, S. P. Chum, A. Hiltner, and E. Baer, "Comparing Elastomeric Behavior of Block and Random Ethylene-Octene Copolymers," *J. Appl. Polym. Sci.* **113**(5), 3236–3244 (2009).
24. Y. S. Hu, V. Prattipati, A. Hiltner, E. Baer, and S. Mehta, "Improving transparency of stretched PET/MXD6 blends by modifying PET with isophthalate," *Polymer (Guildf.)* **46**(14), 5202–5210 (2005).

1. Introduction

In recent years, mechanically tunable miniature coherent laser sources have attracted attention due to their potential applications in integrated spectroscopic devices, including "lab-on-a-chip" designs for sensing and medical applications. Low-cost tunability could open up new applications in display and information processing. In the past, there have been reports of two ways to fabricate such miniature tunable lasers. The earliest mechanically tunable systems involved doping laser dye into cholesteric liquid crystals (CLC), in which the periodic structure forms a stretchable photonic crystal. The lasing action takes place in the reflection band and the corresponding wavelength can be tuned by mechanically changing the pitch length of the CLC elastomer. Such a tunable CLC laser was first demonstrated by Il'chishin *et al.* in 1980 [1] and has been repeated and improved by many other research groups, especially in the last two decades [2–15]. An alternate method has involved UV-light patterning of a rubber photopolymer material. The photoisomerization creates a rubber photonic crystal by periodically changing the refractive indices and thus creating a stretchable photonic crystal. By doping a gain medium into the rubber material, a miniature mechanically tunable rubber laser was demonstrated by Weinberger and others [16–18].

In this paper, we report a method of fabricating an all-polymer mechanically tunable miniature elastomer laser, using a melt-processed, layer-multiplying, process to fabricate a distributed Bragg reflector (DBR) cavity [19–22] co-extruded with a dye-doped skin layer that becomes the active gain layer when folded inside the DBR cavity. The mechanically tunable elastomer laser consists of a dye-doped elastomer gain medium and two elastomer distributed Bragg reflectors. By doping the laser dye in the skin layer, the elastomer multilayer film can be manufactured in a simple roll-to-roll process. The resulting tunable lasers can be cost-effectively and rapidly mass produced from large area sheets of co-extruded polymers.

2. Materials and Processing

Our fabrication procedure closely follows that described in our earlier reports of DBR and distributed feedback (DFB) multilayer laser structures [19–22]. In this work, however, elastomeric polymers are used in order to enable mechanical tunability and the laser dye is contained in a co-extruded skin layer. The elastomer Bragg reflector is based on a pair of semi-crystalline elastomers having crystallinity below 10%. One layer is ethylene-octene (EO) (Dow Engage 8842, $n=1.48$) and the other layer is a fluoroelastomeric terpolymer (THV) (Dyneon THV 220, $n=1.36$) consisting of polyvinylidene fluoride, hexafluoropropylene, and tetrafluoroethylene. The refractive indices were measured by a Metricon 2010 prism coupler using a HeNe gas laser at 633 nm. The multilayer elastomer films were coextruded at 250°C using the continuous layer-multiplying process as reported in Ref [20]. The speed of the chill roll (provided by Randcastle Extrusion Systems, Cedar Grove, NJ) controlled the thickness of the films and the chill roll temperature was maintained at 57°C

using a Sterlco temperature controller from Sterling Inc. (Milwaukee WI). The pump rates of both extruders were kept at $4.5 \text{ cm}^3 \text{ min}^{-1}$, while the skin layer extruder was maintained at $40.5 \text{ cm}^3 \text{ min}^{-1}$.

In order to realize a tunable laser, a suitable fluorescent dye needs to be doped into one or more layers. Unfortunately, the solubility of nearly all fluorescent laser dyes is poor in EO, and worse for THV. For this reason, we chose to utilize a co-extruded skin layer as the active layer incorporating the laser dye. In this case, the skin layer is a polar elastomer in the form of an ethylene terpolymer composed of 40 wt% acrylic ester and glycidyl methacrylate. Its trade name is lotader 8900, and its chemical structure is shown in the inset of the Fig. 1. The lotader elastomer skin layer is doped with 1 wt% Rhodamine 6G perchlorate (R6G) laser dye (molecular weight, MW = 546 g/mole).

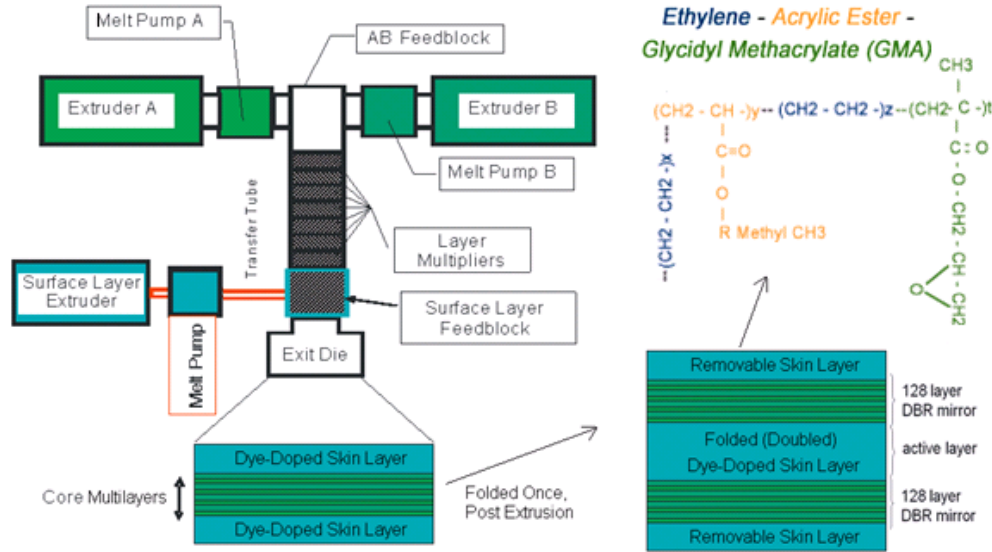


Fig. 1. Schematic of the melt-processing extrusion technique, followed by folding into the stacked structure shown at right.

The co-extruded multilayer elastomer film has a total number of 128 layers with an average layer thickness of $\sim 110 \text{ nm}$ (without stretching) with a layer variation of 25%, which was measured by an atomic force microscope (see Fig. 2(b) below). The extruded skin layers are $15 \mu\text{m}$ in thickness with at least one of the skin layers being doped with R6G laser dye, in order to then serve as the active layer. By simply folding the coextruded film with the dye-doped skin layer in the middle, a distributed Bragg reflector (DBR) elastomer laser film was fabricated. The singly folded DBR elastomer laser film then has a total thickness of about $87 \mu\text{m}$ and an active layer thickness of $30 \mu\text{m}$ and additional skin layers totaling $30 \mu\text{m}$. Layer thickness variations for these films are discussed in [19–22] and below.

3. Experiment

The elastomer laser film was mounted on a uniaxially stretchable translation stage as shown in Fig. 2(a). Transmission spectra were taken using a fiber-coupled Ocean Optics spectrometer, both before and after folding, and at different stretching ratios. The lasing experimental setup is shown in Fig. 2(c). A frequency-doubled Nd:YAG laser was used as the pump source (wavelength – 532 nm , repetition rate – 10 Hz , pulse width – 7 ns , S-polarization). The pump beam, focused by a lens with $f = 10 \text{ cm}$ focal length, was incident at an angle of 20° from normal, allowing the pump light to fully penetrate the DBR reflector, yet avoiding the reflection band. The pump beam size was measured to be about $150 \mu\text{m}$ using a knife edge technique. The lasing emission spectra were also obtained by a fiber-coupled Ocean Optics USB4000 spectrometer. The optical conversion efficiency curve was taken by

integrating the pump spectrum and laser spectrum from the Ocean Optics spectrometer. The laser power was measured by a calibrated photodiode.

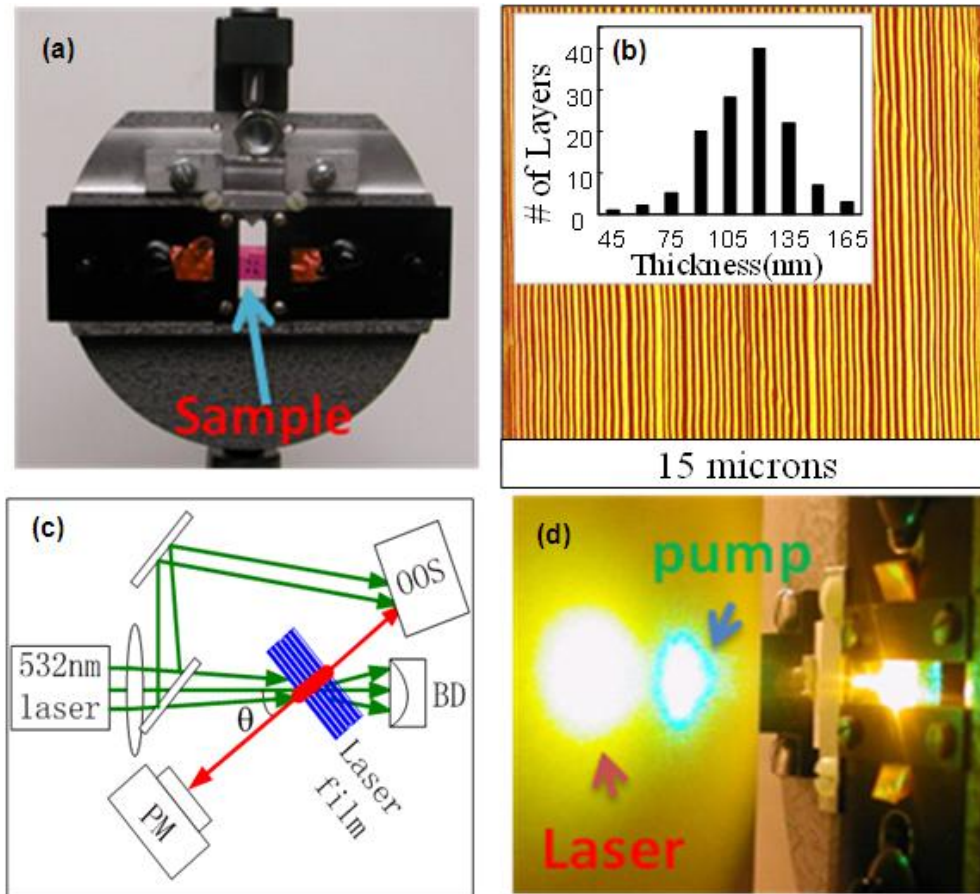


Fig. 2. (a) is the folded elastomeric laser film mounted on the uniaxially stretchable stage; The region marked out by 4 dots locates where the doubled Nd:YAG laser pumped the sample and lasing took place. (b) is an AFM image of the Bragg reflector of the extruded elastomer film with histogram inset showing the layer thickness distribution. (c) is the experiment setup. OOS: fiber-coupled Ocean Optics spectrometer, BD: beam dump, PM: photodiode, $\theta = 20$. (d) is a picture taken while the elastomer laser film was lasing at 600 nm. The left round bright spot is the laser and the right spot is the leftover pump light.

4. Results and discussion

The relationship between the photonic band and the stretching ratio was first studied by stretching the Bragg reflector of the extruded elastomer film from 0 to 150%. Correspondingly, the peak of the photonic band moved from 625nm to 400nm as shown in Fig. 3. These films exhibited an initial small plastic change in their relaxed length upon first being stretched. After the initial stretch and release, however, the stretching and relaxation could usually be repeated over the tuning range of the laser dye (20% strain) many times with no noticeable change in modulus to the limit of the precision of our stretching device. Without stretching, the elastomer film shows negligible birefringence. However, the birefringence increases during stretching [23]. A pseudo-affine model [24] was used to model the shift of the photonic band peak, λ , as a function of the stretching strain, ϵ , and the strain-induced birefringence:

$$\lambda = \lambda_0 \frac{(n_1 + n_2)}{(n_{01} + n_{02})\sqrt{1 + \varepsilon}}$$

where $\varepsilon = (l - l_0)/l_0$, and l_0 and l are the unstretched and stretched lengths, respectively, and λ_0 is the nominal wavelength of the reflection band at zero strain, $n_{01}(n_1)$ and $n_{02}(n_2)$ are the unstretched (stretched) refractive indices in the extrusion direction and perpendicular to the extrusion direction (in our experiment, the uniaxial stretching direction is the same as the extrusion direction) respectively. Our experimental data showed a good agreement with the pseudo-affine model as shown in Fig. 3. In the following lasing experiment, the strain is fairly small ($< 20\%$), as is the induced birefringence $n_1 - n_2 = \Delta n < 0.004$. As a result, the induced birefringence had no noticeable effect on the photonic bands quality in either polarization direction, nor, therefore, on the lasing action.

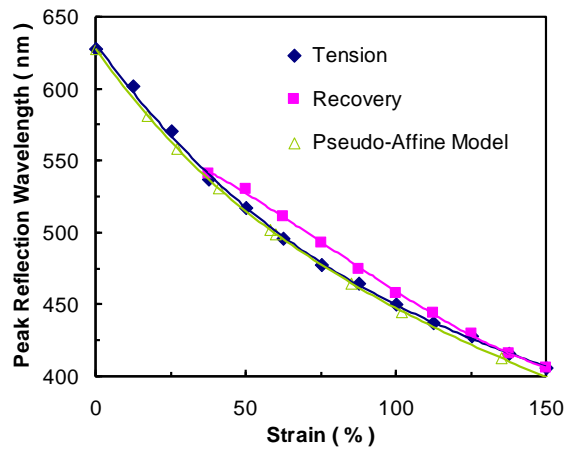


Fig. 3. Shift of photonic band peak vs. the stretching strain. The blue diamond dots and the pink square dots are the experimental data for stretching and recovery, respectively, and the triangle dots are the calculated results using a pseudo-affine Model.

In the laser experiment, the length of the unstretched laser film is 9 mm and the reflection band and the lasing wavelength are both located at 614 nm. By stretching it from 0% to 19%, the photonic band center shifts from 614 to 565 nm. The lasing wavelength is a function of both the broad emission spectrum of the R6G dye and the location of the optimal reflection band wavelength of the multilayer cavity mirrors, which can be found by treating the multilayers as a simple quarter-wavelength stack. The laser emits from both sides normal to the surface. Bright emission was observed as shown in Fig. 2(d). The left round bright spot on a piece of white paper is the generated tunable laser light and the right spot nearby is the unconverted 532 nm pumping light. The lasing was observed at defect states (i.e., local transmission maxima inside the spectral reflection band) as shown in Fig. 4(a). The transmission spectrum (black curve in Fig. 4(a)) is the convolution of the absorption band of R6G laser dye (450-560 nm) and the photonic reflection bands of the two elastomer distributed Bragg reflectors (580-650 nm). At zero strain, the films lased at two wavelengths, 614 nm and 587 nm, the former as expected for the dominant reflection band structure and the latter probably due to reflection band defects arising from variations in the layer thicknesses. (See [19–22].) As the films were stretched so that the reflection band shifted towards the peak dye fluorescence spectrum, the weaker lasing emission disappeared and single wavelength emission was observed as shown in Fig. 4(b), which shows the typical emission spectra below and above the lasing threshold. The inset to Fig. 4(b) shows the typical optical conversion efficiency curve at 600 nm, in which the lasing threshold can be observed and the optical conversion efficiency is found to be about 0.8% in the lasing region.

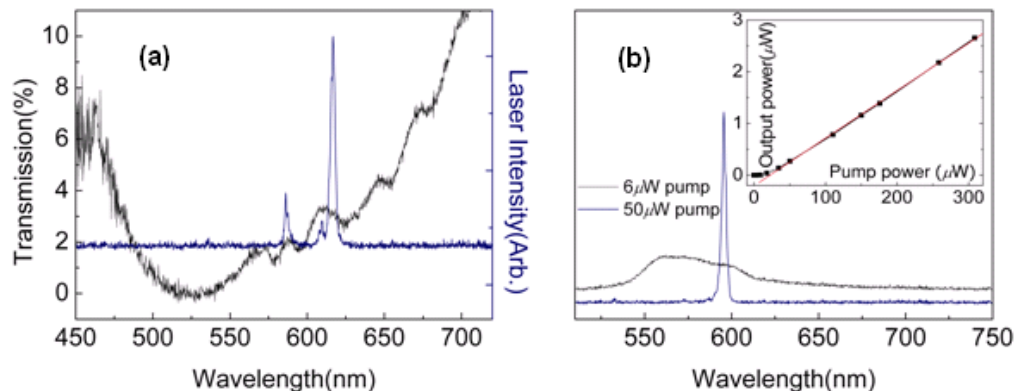


Fig. 4. (a) Transmission and emission spectra of the folded unstretched elastomer laser film. (b) The emission spectrum at specified pump powers below and above the lasing threshold. Note: the vertical axes for the two curves are not to the same scale. The curve in the inset shows the optical conversion efficiency at 600nm.

Continuous wavelength tuning from red to green was observed by stretching the laser film as shown in Fig. 5. The series of curves in Fig. 5(a) (top) are the transmission curves corresponding to stretching the extruded film (before folding) from 0% to 19%. The series of curves in Fig. 5(a) (top) are the transmission curves of the coextruded film at different stretching ratios. Two local minima in the transmission spectrum can be seen. The stationary minimum below 550 nm is due to the absorption band of R6G laser dye while the shifting longer wavelength minima indicate the photonic reflection band of the elastomer distributed Bragg reflectors. The series of curves in Fig. 5(b) (bottom) show the laser output at different wavelengths for a folded laser film over the same stretching range illustrated in Fig. 5(a). In our experiment, when pumped by a fixed power (about 50 μW), the intensity of the laser first increases and then decreases as the tuning wavelength changes from 614 nm to 565 nm, as shown, which is consistent with the trend in the R6G gain curve (the dark wine colored curve in Fig. 5(b)). The highest laser intensity was observed at about 595 nm, which is somewhat longer than the peak of the R6G gain curve, which peaks at about 575 nm. There are at least three possible contributions to this shift in the peak of the gain curve: (1) re-absorption of laser light on the blue side by the R6G laser dye itself (the black curve in Fig. 5(b)); (2) a decrease of the amount of dye inside the focal volume during stretching due to thinning of the layers; (3) a decrease in the reflectance of the Bragg reflector (see Fig. 5(a)) which becomes slightly shallower and narrower during stretching. The spectral width of the laser was measured to be about 2nm at full width half maximum (FWHM).

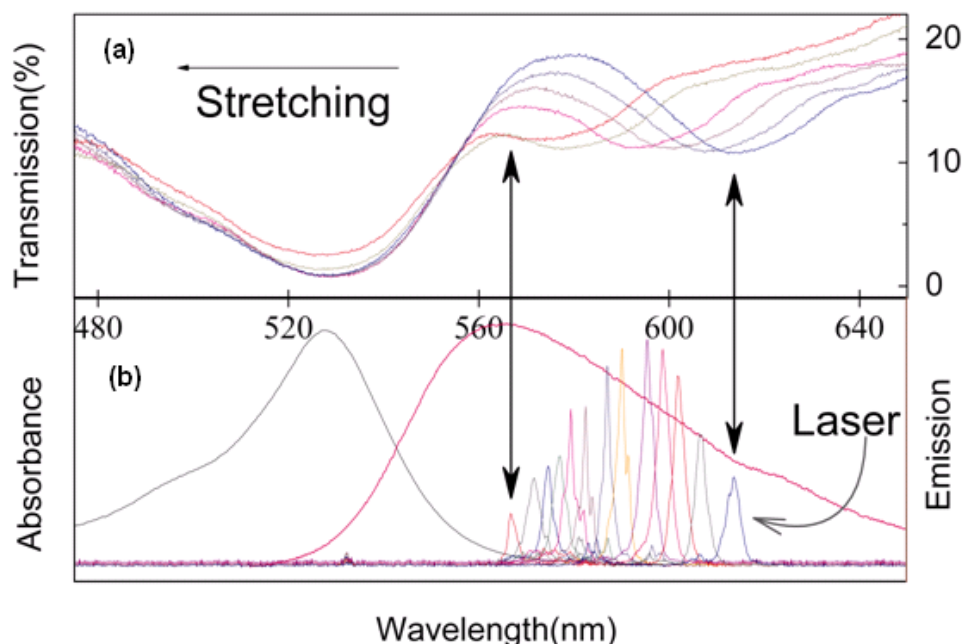


Fig. 5. Absorbance, emission, tuning transmission and tuning emission spectra of the tunable DBR elastomer laser. The series of curves in (a) (top) are the transmission curves of a single extruded film while stretching from 0% to 19%. The series of curves in (b) (bottom) are the output laser wavelength at different stretching ratios for the folded laser film. In (b), the black and the pink colored curves are the absorbance and emission spectra of the R6G laser dye doped in lotader elastomer polymer.

As shown by the transmission spectrum in Fig. 5(a), the photonic reflection band for the Bragg reflector is very broad; however, the lasing spectrum is much narrower (~ 2 nm in full width half maximum) as shown in Fig. 5(b). Lasing at defect states has been observed and reported previously [22] with these materials. Such phenomenon can be explained by the gain enhancement at the defect state in the photonic reflection band. The presence of defect states is important for controlling the lasing wavelength and narrowing the spectral width. Such defect states can be due to the random variations of the layer thickness of the Bragg reflector or by intentionally introducing a defect layer in the Bragg reflector. Defect states in the reflection band are thus preferred in that they not only control the lasing wavelength and spectrum width, but they also enhance the overall lasing gain resulting in lowering the lasing threshold and increasing the optical conversion efficiency.

In summary, we described a mechanically tunable all-polymer surface emitting micro-resonator dye laser with distributed Bragg reflectors. These lasers are produced entirely by a melt-process that would enable high-throughput roll-to-roll production methods. These lasers were repeatedly tunable over an approximate 50 nm range by uniaxial stretching. Lasing was observed at defect states within the reflection band. The presence of these defects led to lower observed thresholds and greater efficiency as well as more easily controlled tunability.

Acknowledgments

The authors are grateful to the National Science Foundation for financial support under the Science and Technology Center for Layered Polymeric Systems under grant number DMR 0423914. Youngstown State University acknowledges the contribution of the State of Ohio, Department of Development, State of Ohio, the Chancellor of the Board of Regents and Third Frontier Commission, which provided funding in support of the Research Cluster on Surfaces in Advanced Materials.